



ELSEVIER

Available online at www.sciencedirect.com

ScienceDirect

journal homepage: www.elsevier.com/locate/he

CrossMark

Monodisperse nickel–palladium alloy nanoparticles supported on reduced graphene oxide as highly efficient catalysts for the hydrolytic dehydrogenation of ammonia borane

Nesibe Sedanur Çiftci, Önder Metin *

Department of Chemistry, Faculty of Science, Atatürk University, Erzurum 25240, Turkey

ARTICLE INFO

Article history:

Received 4 August 2014

Received in revised form

27 August 2014

Accepted 10 September 2014

Available online 3 October 2014

Keywords:

Nickel

Palladium

Alloy nanoparticles

Reduced graphene oxide

Ammonia borane

Dehydrogenation

ABSTRACT

Addressed herein is the catalysis of reduced graphene oxide-supported monodisperse NiPd alloy nanoparticles (NPs) (rGO-NiPd) in the hydrolytic dehydrogenation of ammonia borane (AB). This is the first example of the use of NiPd alloy NPs as catalyst in the hydrolytic dehydrogenation of AB. Monodisperse NiPd alloy NPs (3.5 nm) were synthesized by co-reduction of nickel(II) acetate and palladium(II) acetylacetonate in oleylamine (OAm) and borane-*tert*-butylamine complex (BTB) at 100 °C. The current recipe allowed to control the composition of NiPd alloy NPs and to study the composition-controlled catalysis of rGO-NiPd in the hydrolytic dehydrogenation of AB. Among the all compositions tested, the Ni₃₀Pd₇₀ was the most active one with the turnover frequency of 28.7 min⁻¹. The rGO-Ni₃₀Pd₇₀ were also durable catalysts in the hydrolytic dehydrogenation of AB providing 3650 total turnovers in 35 h and reused at six times without deactivation. The detailed reaction kinetics of hydrolytic dehydrogenation of AB revealed that the reaction proceeds first order with respect to the NiPd concentration and zeroth order with respect to the AB concentration. The apparent activation energy of the catalytic dehydrogenation of AB was also calculated to be $E_a^{app} = 45 \pm 2 \text{ kJ}^* \text{mol}^{-1}$.

Copyright © 2014, Hydrogen Energy Publications, LLC. Published by Elsevier Ltd. All rights reserved.

Introduction

Hydrogen has been considered to be an alternative energy vector for almost two decades, but it is now in many of our daily life applications owing to the recent advances in nanoscience, catalysis, modeling and bio-inspired approaches that offer new research prospects for a variety of

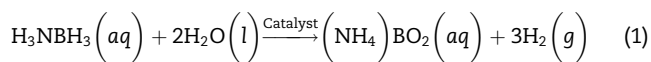
hydrogen and fuel cell technologies. However, hydrogen storage is still a crucial technology for the advancement of hydrogen and fuel cell power technologies in transportation, stationary and portable applications [1]. Although several hydrogen storage technologies such as compressing gaseous hydrogen are available for mobile systems nowadays, the desired technical requirements have not been accomplished yet. Therefore, the

* Corresponding author. Tel.: +90 442 231 4410; fax: +90 442 236 0948.

E-mail addresses: ometin@atauni.edu.tr, ondermetin1981@hotmail.com (Ö. Metin).
<http://dx.doi.org/10.1016/j.ijhydene.2014.09.060>

0360-3199/Copyright © 2014, Hydrogen Energy Publications, LLC. Published by Elsevier Ltd. All rights reserved.

development of high capacity, efficient and safe hydrogen storage technologies are required [2]. In this respect, several promising storage technologies have been investigated such as chemical hydrogen storage, storing hydrogen within a compound via chemical bond. Among the chemical hydrogen storage materials have been tested so far [3], ammonia borane ($\text{H}_3\text{N}\cdot\text{BH}_3$, AB) is the leading candidate owing to its stability in air and solution, very high hydrogen content (19.6 wt%) with a system-level H_2 energy storage density of about 2.74 kWh/L (two times higher than DOE's 2017 target, 1.3 kWh/L [2]), and other desirable chemical properties [4]. The hydrogen stored in AB can be generated via several ways (solid state thermolysis [5], dehydrocoupling [6] and dehydrogenation via solvolysis [7]) among which the catalytic hydrolysis (Eq. (1)) appeals to be the most favorable one for mobile applications owing to its favorable technical advantages such as fast hydrogen release and to be performable at low temperatures [8].



Up to date, many transition metals (Fe [9], Co [10], Ni [11], Cu [12], Pd [13], Ru [14], Pt [15]) or their bimetallic counterparts (NiRu [16], NiFe [17], CuRu [18], CoNi [19], PdPt [20], NiPt [21], CoFe [22], CuFe [23]) have been presented to catalyze the hydrolytic dehydrogenation of AB. Among these catalysts, nickel, cobalt and palladium were emerged to be the most effective ones. In our recent studies, we have reported that monodisperse Ni nanoparticles (NPs) supported on Ketjen carbon [24] and Pd NPs supported on reduced graphene oxide [25] were highly efficient catalysts for the hydrolysis of AB under ambient conditions. Additionally, we have demonstrated that monodisperse CoPd alloy NPs were more efficient catalysts than single Pd NPs owing to the synergistic effect between two distinct metals [26]. Xu and co-workers have also reported the synergistic catalysis of bimetallic Ni-based NPs in the hydrolysis of AB [27]. However, a literature search was resulted in no example of bimetallic NiPd alloy catalysts in the hydrolysis of AB. These results motivated us to study the catalysis of monodisperse NiPd alloy NPs for the hydrolysis of AB.

We report herein the catalysis of reduced graphene oxide-supported monodisperse NiPd alloy nanoparticles (NPs) (rGO-NiPd) in the hydrolytic dehydrogenation of AB. To the best of our knowledge, this is the first example of the use of NiPd alloy NPs as catalyst in the hydrolytic dehydrogenation of AB. 3.5 nm NiPd alloy NPs were synthesized by co-reduction of nickel(II) acetate and palladium(II) acetylacetonate in oleylamine (OAm) and borane-*tert*-butylamine complex (BTB) [28]. The composition of NiPd alloy NPs was easily tuned by changing the metal precursor ratio. Next, as-prepared NiPd alloy NPs were supported on rGO (rGO-NiPd) via simple liquid impregnation method and tested in the hydrolytic dehydrogenation of AB without any special treatment to remove the surfactants. Among the three compositions of NiPd alloy NPs tested, the $\text{Ni}_{30}\text{Pd}_{70}$ showed the best performance with the initial turnover frequency (TOF) of 28.7 mol H_2 min^{-1} . The reaction kinetics of rGO-Ni₃₀Pd₇₀ catalyzed hydrolytic dehydrogenation of AB was studied by depending on the catalyst concentration, substrate concentration and temperature.

Experimental

Materials

Nickel(II) acetate tetrahydrate ($\text{Ni}(\text{ac})_2\cdot 4\text{H}_2\text{O}$, 98%), palladium(II) acetylacetonate ($\text{Pd}(\text{acac})_2$), oleylamine (OAm, >70%), borane-*tert*-butylamine (BTB, 97%), 1-octadecene (tech. grade, 90%), hexanes (99%), borane–ammonia complex (AB, 97%), potassium permanganate (KMnO_4 , >99%), sodium nitrate (NaNO_3 , >99%), and dimethylformamide (DMF, >99%) were purchased from Sigma–Aldrich® and used as received. Hydrogen peroxide (H_2O_2 , 30%) and sulfuric acid (H_2SO_4 , 95–98%) were purchased from Merck®. Natural graphite flakes (average particle size 325 mesh) were purchased from Alfa Aesar®. Deionized water was distilled by water purification system (Milli-Q System). All glassware and Teflon-coated magnetic stir bars were cleaned with acetone, followed by copious rinsing with distilled water before drying at 150 °C in oven for overnight.

Characterizations

Transmission electron microscope (TEM) images were obtained by using FEI Tecnai G² Spirit BioTwin High-Contrast microscope instrument operating 120 kV. X-ray diffraction pattern (XRD) was recorded on a Rigaku Miniflex diffractometer with $\text{CuK}\alpha$ (30 kV, 15 mA, $\lambda = 1.54051 \text{ \AA}$), over a 2θ range from 10 to 80° at room temperature. The metal content of the NiPd alloy NPs and rGO-NiPd catalysts was determined by using Leiman series inductively coupled plasma-mass spectroscopy (ICP-MS) after each sample was completely dissolved in aqua-regia (HNO_3/HCl : 1/3 v/v ratio). ¹¹B NMR spectrum was measured on a Bruker Avance DPX 400 MHz spectrometer (128.2 MHz for ¹¹B NMR).

Synthesis of reduced graphene oxide

rGO was prepared by using a well-established two step procedure; (i) the synthesis of graphite oxide via modified Hummer's method [29] and (ii) the reduction of graphite oxide by refluxing its DMF solution for 6 h [30]. The details of the rGO synthesis procedure and the characterization of rGO can be found in our recent reports [31].

Synthesis of monodisperse NiPd alloy nanoparticles and supporting them on reduced graphene oxide

The monodisperse NiPd alloy NPs were synthesized by using our established protocol with minor modifications [28]. In a typical synthesis of Ni₃₀Pd₇₀ NPs, nickel(II) acetate tetrahydrate (0.2 mmol) and palladium(II) acetylacetonate (0.2 mmol) were dissolved in 3 mL of OAm in a 20 mL of glass vial. In a four-necked glass reactor that allows to study under inert atmosphere, 200 mg of BTB was dissolved in 3 mL of OAm and 7 mL of 1-octadecene at 100 °C under magnetic stirring. Next, the metal precursor mixture was quickly injected into the reactor under argon environment. The reaction was then proceed for 1 h before cooled down to room temperature. Then, the colloidal NPs mixture was transferred into two

Download English Version:

<https://daneshyari.com/en/article/7717493>

Download Persian Version:

<https://daneshyari.com/article/7717493>

[Daneshyari.com](https://daneshyari.com)